RESEARCH PAPER

In Silico Evaluation of Bioactive Compounds from Amorphophallus Paeoniifolius Ethanolic Tuber Extract as Potential Therapeutics for PCOS: Molecular Docking, ADMET, and Pass Prediction Analysis

N.P. Sreesaila[1], O.S. Nimmi[1*], P Ruban[2], and Sameena Yousuf[3]

[1]*Department of Biotechnology, Nehru Arts and Science College, Coimbatore - 641105, Tamil Nadu, India*
[1*]*Department of Biotechnology, Nehru Arts and Science College, Coimbatore - 641105, Tamil Nadu, India*
[2]*Department of Biotechnology, Nehru Arts and Science College, Coimbatore - 641105, Tamil Nadu, India*
[3]*Department of Science and Humanities, Nehru Institute of Engineering and Technology, Coimbatore - 641114, Tamil Nadu, India*
***Corresponding author:** N.P Sreesaila*
sailakedaram@gmail.com

Received: 16th Dec, 2025; Revised: 8th Feb 2026; Accepted: 12th Feb, 2026; Available Online: 30th March, 2026

ABSTRACT
Polycystic ovary syndrome (PCOS) is a prevalent endocrine and metabolic disorder with limited safe therapeutic options. This study investigated the ethanolic tuber extract of Amorphophallus paeoniifolius for its phytochemical composition, molecular interactions with PCOS-associated targets, pharmacokinetic properties, and therapeutic potential using in silico approaches. Qualitative screening revealed the presence of alkaloids, tannins, phenols, flavonoids, and carbohydrates. GC–MS analysis identified 21 bioactive compounds, including linoleic acid, cis-vaccenic acid, palmitic acid ethyl ester, stigmasterol, and β-sitosterol. Molecular docking demonstrated that linoleic acid and cis-vaccenic acid exhibited strong binding affinities (–6.0 to –5.2 kcal/mol) with key PCOS-related proteins, comparable to standard drugs such as metformin and clomiphene citrate, while steroidal compounds displayed moderate interactions. ADMET analysis highlighted cis-vaccenic acid as the most pharmacokinetically favorable compound, with high gastrointestinal absorption, optimal lipophilicity, good bioavailability, and minimal metabolic liabilities. Toxicity predictions confirmed safety, and PASS analysis suggested multifunctional activity, including antidiabetic, antiviral, and antimutagenic properties. Overall, cis-vaccenic acid emerges as a promising natural lead compound with strong target affinity, favorable pharmacokinetics, and a safety profile, supporting further experimental evaluation for the management of PCOS and related metabolic disorders.
Keywords: *Amorphophallus paeoniifolius, cis-Vaccenic acid, Polycystic ovary syndrome (PCOS), Molecular docking, ADMET, and PASS prediction*
How to cite this article: Sreesaila NP, Nimmi OS, Ruban P, Yousuf S, In Silico Evaluation Oof Bioactive Compounds from Amorphophallus Paeoniifolius Ethanolic Tuber Extract As Potential Therapeutics for Pcos: Molecular Docking, Admet and Pass Prediction Analysis. Int J Drug Deliv Technol. 2026;16(3): 214-233. DOI: 10.25258/ijddt.16.3.28 **Source of support:** Nil.
Conflict of interest: None

INTRODUCTION

Polycystic ovary syndrome (PCOS) is a multifactorial endocrine disorder affecting 6–20% of women of reproductive age, making it one of the most prevalent causes of infertility worldwide [1, 2]. The condition is characterized by chronic anovulation, hyperandrogenism, and polycystic ovarian morphology, which collectively contribute to menstrual irregularities, metabolic dysfunction, and subfertility [3, 4]. The pathophysiology of PCOS involves complex interactions among genetic, hormonal, metabolic, and environmental factors that disrupt normal ovarian and endocrine signaling [5, 6]. Metabolic abnormalities, including insulin resistance, dyslipidemia, and low-grade chronic inflammation, are central to PCOS pathogenesis [7, 8]. Elevated insulin levels stimulate ovarian theca cells to overproduce androgens, which, in turn, impair follicular maturation and ovulation [9]. Moreover, inflammatory signaling pathways such as those mediated by Toll-like receptor 4 (TLR4), prostaglandin-endoperoxide synthase 2 (PTGS2/COX-2), and transcription factor early growth response protein 1 (EGR1) are implicated in PCOS-related ovarian dysfunction,

oxidative stress, and abnormal steroidogenesis [10, 11]. These pathways collectively contribute to follicular arrest, ovarian fibrosis, and metabolic dysregulation characteristic of PCOS.

Although pharmacological therapies such as clomiphene citrate for ovulation induction and metformin for insulin sensitization remain the mainstay of PCOS management, these drugs are often limited by side effects and suboptimal response rates [12, 13]. Long-term administration of clomiphene citrate has been associated with ovarian hyperstimulation and reduced endometrial receptivity, while metformin use is linked to gastrointestinal discomfort and potential hepatotoxicity [14, 15]. Consequently, there is a pressing need to identify safer, more effective, and naturally derived therapeutic alternatives that target the underlying molecular mechanisms of PCOS.

In recent years, the exploration of phytochemicals for the management of PCOS and related metabolic disorders has gained significant attention. Plant-derived compounds often exhibit a wide range of biological activities, including antioxidant, anti-inflammatory, insulinsensitizing, and hormone-modulating effects [16, 17]. Phytotherapeutic agents are considered advantageous because they act synergistically on multiple signaling pathways, thereby restoring hormonal and metabolic homeostasis [18]. Moreover, their safety profiles and low toxicity make them suitable for long-term use compared to synthetic drugs.

Amorphophallus paeoniifolius (Dennst.) Nicolson, commonly known as elephant foot yam, belongs to the family Araceae and is widely distributed in tropical regions of Asia and Africa. The tuber of *A. paeoniifolius* is traditionally consumed as a food source and used in Ayurvedic and folk medicine to treat a variety of ailments including inflammation, dysentery, hemorrhoids, and hormonal disorders [19, 20]. Ethnobotanical evidence suggests that the plant possesses rejuvenating and restorative properties that may benefit reproductive and metabolic health [21]. Phytochemical investigations of *A. paeoniifolius* have reported the presence of a diverse array of secondary metabolites such as flavonoids, alkaloids, saponins, steroids, terpenoids, tannins, and phenolic compounds [22]. Notably, fatty acids such as linoleic acid and cis-vaccenic acid, commonly found in *A. paeoniifolius*, have been shown to modulate inflammatory pathways and improve insulin sensitivity [23]. Such properties suggest that *A. paeoniifolius* may have therapeutic potential in alleviating the pathophysiological mechanisms underlying PCOS.

Despite these promising bioactivities, the molecular mechanisms through which *A. paeoniifolius* exerts its pharmacological effects remain largely unexplored. The integration of experimental phytochemical profiling with computational approaches, such as molecular docking and molecular dynamics (MD) simulations, provides a robust framework for identifying bioactive compounds that interact with disease-associated target proteins [24, 25]. These *in silico* methods enable the prediction of binding affinities, stability, and conformational dynamics of ligand–protein interactions, thereby offering valuable insights into potential therapeutic mechanisms before experimental validation [26].

Among the molecular targets associated with PCOS, Tolllike receptor 4 (TLR4) plays a key role in the recognition of inflammatory stimuli and activation of downstream NFκB signaling pathways that exacerbate ovarian inflammation and insulin resistance [10]. Similarly, prostaglandin-endoperoxide synthase 2 (PTGS2/COX-2) is a critical enzyme in prostaglandin biosynthesis, influencing ovulatory processes and inflammatory responses within the ovary [11]. Early growth response protein 1 (EGR1), a zinc-finger transcription factor, is involved in folliculogenesis, steroidogenic regulation, and endometrial receptivity [27]. Dysregulation of these proteins has been implicated in PCOS-associated ovarian dysfunction, suggesting that their modulation by natural compounds could restore normal ovarian physiology [28].

Recent advances in bioinformatics and cheminformatics have facilitated the rapid screening of natural compounds for their drug-likeness and pharmacokinetic properties through platforms such as SwissADME and ProTox-II [29, 30]. Furthermore, the Prediction of Activity Spectra for Substances (PASS) online tool enables the evaluation of the biological potential of compounds based on structure–activity relationships, providing an efficient means of identifying multifunctional therapeutic candidates [31]. These computational techniques collectively reduce the time and cost associated with traditional drug discovery, enabling the rational selection of phytochemicals for disease-specific applications [32].

In this study, the bioactive potential of *Amorphophallus paeoniifolius* tuber against PCOS-associated target proteins was investigated using a comprehensive *in silico* approach. Phytochemical profiling of the tuber extract was performed using Gas Chromatography–Mass
Spectrometry (GC–MS), leading to the identification of major constituents. Based on abundance and reported biological relevance, lactone, 9,12-octadecadienoic acid

*Author for Correspondence: sailakedaram@gmail.com

(linoleic acid), and cis-vaccenic acid were selected for further analysis. These phytocompounds were subjected to molecular docking studies against key PCOS-related proteins, namely TLR4, PTGS2 (COX-2), and EGR1, to evaluate their binding affinities and interaction profiles. The standard drug metformin was included for comparative assessment of binding efficiency. Furthermore, ADMET and PASS analyses were conducted to predict pharmacokinetic properties, toxicity, and potential biological activities of the selected compounds. This integrative approach provides mechanistic insights into the therapeutic potential of *A. paeoniifolius* phytochemicals in PCOS management and lays the foundation for future *in vitro* and *in vivo* validation studies.

MATERIALS AND METHODS Sample Collection

Fresh tubers of *A. paeoniifolius were* collected from Mullurkkara, Thrissur District, Kerala, India (latitude: 10.7847°; longitude: 76.2581°). Healthy, undamaged tubers were selected for the study. The plant was identified and authenticated by experts at the Botanical Survey of India (BSI), Tamil Nadu. A voucher specimen (BSI/SRC/5/23/2016/Tech/230) was deposited and preserved for future reference.

Sample Preparation and Extraction

The tubers were washed, cut into small pieces, shadedried, and ground into fine powder using a laboratory mill. The powdered material was stored in a desiccator until use. Extraction was carried out using Soxhlet apparatus with ethanol, petroleum ether, and hexane through hot percolation. The resulting extracts were filtered through Whatman No. 1 filter paper and concentrated by evaporation at room temperature until dryness. Dried extracts were stored in airtight containers at 4 °C for further analysis.

Phytochemical Screening

The preliminary phytochemical screening of the extracts of *A. paeoniifolius* tuber was carried out to detect major classes of bioactive compounds, including alkaloids, flavonoids, terpenoids, phenols, tannins, steroids, saponins, and carbohydrates. Standard procedures described by Oloyede *et al*. [33].

GC-MS Analysis of the Extract

The ethanol extract of *A. paeoniifolius* tuber was subjected to Gas Chromatography–Mass Spectrometry (GC–MS) analysis to determine its bioactive volatile constituents. The extract was filtered through a 0.2 µm nylon syringe filter (13 mm) and transferred into a clean GC–MS vial prior to injection. GC–MS analysis was carried out using an Agilent Technologies 7890A gas chromatograph coupled with a 5975C triple-axis mass selective detector. Separation of compounds was achieved on a DB-5MS capillary column (30 m × 0.25 mm i.d., 0.25 µm film thickness). The injector temperature was maintained at 280 °C, and a 2 µL aliquot of the sample was injected in splitless mode. High-purity helium (99.9995%) was used as the carrier gas at a constant flow rate of 1 mL/min. The oven temperature was programmed with an initial temperature of 40 °C (held for 3 min), which was then increased at a rate of 20 °C/min to 280 °C and held for 5 min. The mass spectrometer was operated in electron ionization (EI) mode at 70 eV. The chemical constituents were identified by comparing the obtained mass spectra with those in the NIST 08 mass spectral library.

Collection of Compounds

The dataset used in this study consisted of 21 compounds identified from the ethanolic extract of *A. paeoniifolius* tuber through GC–MS analysis. Among these, three compounds were selected for further analysis based on their predicted interactions with polycystic ovary syndrome (PCOS)-associated target proteins and their pharmacological relevance when compared with the standard drugs Metformin and Clomiphene Citrate. The study evaluated the phytochemical profile of the ethanolic extract of *A. paeoniifolius* using GC–MS and employed molecular docking approaches to identify the most promising bioactive compounds targeting key proteins involved in PCOS related protein.

Software and hardware

The RCSB Protein Data Bank (https://www.rcsb.org) and the PubChem database (https://pubchem.ncbi.nlm.nih.gov) were used in this investigation. Utilizing PyRx and AutoDock Vina 0.8 (Dallakyan and Olson, 2015) software or, alternatively, using the BIOVIA Discovery Studio (RRID:SCR_015651) protein visualizer (Pawar and Rohane, 2021).

Preparation of Protein

The crystal structures of PCOS-related proteins TLR4 (PDB ID-3FXI), PTGS2 (PDB ID : 5F19) and EGR1 (PDB ID- 4X9J) were sourced from the RCSB Protein Data Bank (PDB) (https://www.rcsb.org/) to facilitate docking studies **(Fig. 1a** to **c).** Preparing a selected protein involves altering its macromolecular structure to establish a more suitable arrangement for conducting a computational experiment [34].

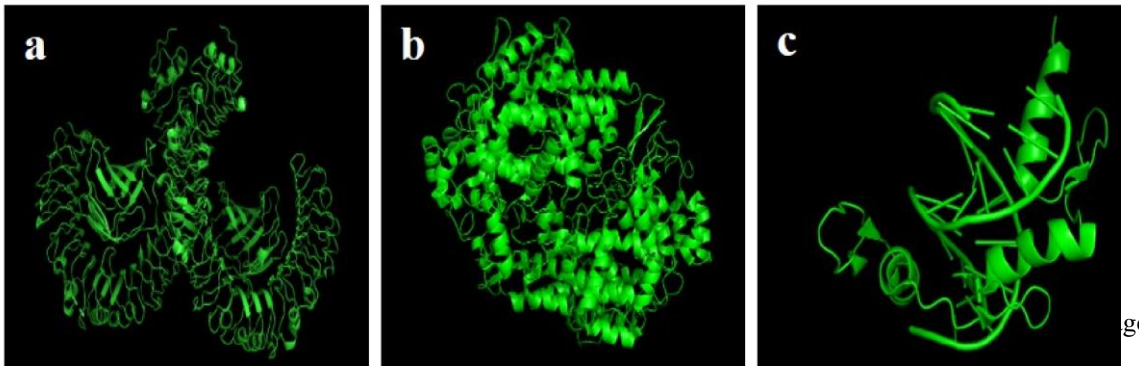

Fig. 1. 3D structure representation of PCOS-related proteins, (a) TLR4 (PDB ID-3FXI), (b) PTGG2 (PDB ID: 5F19) and (c) EGR1 (PDB ID- 4X9J)

Preparation of Ligands

The structures of three identified compounds obtained through GC-MS analysis of the ethanolic extract of *A. paeoniifolius* along with the standard drug. The Lactone G (γ-Butyrolactone) (PubChem ID: 7302)**,** 9,12Octadecadienoic acid (Z, Z) (Linoleic acid) (CID: 5280450)**,** and cis-Vaccenic acid (CID: 5282761) were researched and identified in the PubChem database (https://pubchem.ncbi.nlm.nih.gov/). The 3D conformations of the ligands and the standard drug, Metformin (PubChem CID -4091) were obtained. Ligands are utilized to investigate their potential interactions with the of PCOS-related proteins, TLR4 (PDB ID-3FXI), PTGS2 (PDB ID - 5F19), and EGR1 (PDB ID- 4X9J) through site-specific molecular docking. All structures were analyzed using PLIP v1.1.1. PLIP facilitates thorough detection and visualization of protein-ligand interaction patterns

Molecular Docking Analysis

Molecular docking studies were performed to evaluate the interaction potential of the bioactive compounds identified through GC–MS analysis with polycystic ovary syndrome (PCOS)-related target proteins, which play key roles in the progression of the disorder [35]. The preparation of ligands and receptor proteins was carried out using AutoDock tools, where the structures were converted into the PDBQT file format. Docking simulations were executed using AutoDock Vina to predict the binding affinity and orientation of the ligands within the active sites of the target proteins. A rigid-flexible docking approach was employed, with each receptor kept rigid while allowing full flexibility of the ligands. The grid box parameters were defined to encompass the active site residues of each receptor, and the specific grid coordinates used for each protein are provided in **Table 1**. The binding affinities were expressed as binding energies in kilocalories per mole (kcal/mol), where lower (more negative) values indicated stronger and more stable ligand–protein interactions [36]. Post-docking analyses were performed using BIOVIA Discovery Studio Visualizer, which facilitated detailed visualization of the molecular interactions, including hydrogen bonding, hydrophobic contacts, and other non-covalent interactions between the ligand and receptor residues. The same docking protocol was applied to the standard drugs, Metformin and Clomiphene Citrate, to enable comparative evaluation of binding efficiencies and interaction profiles with the selected PCOS target proteins.

Table 1 Grid box parameters selected for PCOS related target protein, based on the binding site residues

PDB ID	Active Site Residues	Grid Box Parameter	
3FXI	LEU54, ILE80, VAL2, LEU 87, PHE126, SER127, TYR 131, SER141, ILE153	11.248 X -5.270 X -5.104	60 X60 X 60
5F19	ALA202, HIS207, LEU381, ASN382, HIS386, TRP387, HIS388	22.594 X 40.999 X 39.56	60 X60 X 60
4X9J	LEU88, LEU222, VAL223, HIS226, TYR248, PRO255	-4.297 X -20.219 X -21.261	60 X60 X 60

Drug-Likeness, ADMET, and *in silico* PASS Prediction Analysis

It was essential to evaluate the drug-likeness and ADMET (Absorption, Distribution, Metabolism, Excretion, and Toxicity) profiles of the selected compounds to minimize potential time and resource inefficiencies during subsequent analyses [32]. The drug-likeness properties of the selected ligand molecules were assessed *in silico* using the SwissADME web tool (http://www.swissadme.ch/). The evaluated parameters included molecular weight (MW ≤ 500 Da), octanol–water partition coefficient (iLOGP), number of hydrogen bond donors (HBD ≤ 5), number of hydrogen bond acceptors (HBA ≤ 10), topological polar surface area (TPSA), and number of rotatable bonds (nROT) [37]. The SwissADME platform analyzed these molecular descriptors by converting the uploaded SDF file of each ligand into SMILES format and calculating physicochemical and pharmacokinetic properties based on Lipinski's Rule of Five (RO5) [38].

The toxicity profiles of the selected compounds were further predicted using the ProTox-II server (https://toxnew.charite.de/protox_II/) [30]. This web-based tool classifies compounds according to their potential toxicological endpoints, such as hepatotoxicity, carcinogenicity, mutagenicity, and cytotoxicity, thereby providing a comprehensive overview of their safety characteristics.

In the present investigation, the pharmacological activity of the principal bioactive components identified from *A. paeoniifolius* was evaluated using the Prediction of Activity Spectra for Substances (PASS) online tool [17]. The molecular structures of the compounds were first converted into SMILES (Simplified Molecular Input Line Entry System) format using ChemDraw, and subsequently analyzed in the PASS online application to predict their probable activity (Pa) and probable inactivity (Pi) values [39, 31]. Compounds with higher *Pa* values were considered to possess a greater likelihood of exhibiting the predicted biological activity.

RESULTS AND DISCUSSION Qualitative Phytochemical Analysis

The qualitative phytochemical screening of the ethanol extract of *A. paeoniifolius* revealed the presence of key secondary metabolites (**Table 2**). Alkaloids and tannins were strongly detected through Dragendorff's and ferric chloride tests, while phenols and carbohydrates showed

moderate intensity in the lead acetate and Molisch assays. A weak reaction for flavonoids was noted, whereas terpenoids, steroids, and saponins were absent based on negative Salkowski, Liebermann–Burchard, and frothing tests. The presence of alkaloids, tannins, phenols, and flavonoids indicates that the species contains bioactive constituents with potential therapeutic relevance. This finding aligns with earlier reports documenting a wide spectrum of phytochemicals in *A. paeoniifolius*, including alkaloids, flavonoids, steroids, tannins, carbohydrates, reducing sugars, amino acids, glycosides, saponins, phenols, and glucomannans [40, 41]. Sen *et al*. [42] further demonstrated that aqueous extracts predominantly contain alkaloids, flavonoids, reducing sugars, carbohydrates, and tannins, while ethanolic extracts additionally exhibit steroids and triterpenoids. The plant's diverse phytochemical profile supports its broad therapeutic potential. As highlighted by Sharma and Kumar [43], *A. paeoniifolius* exhibits multiple pharmacological activities, These bioactive components substantiate its traditional including antioxidant, antimicrobial, anticancer, medicinal applications and justify further pharmacological gastroprotective, antidiabetic, anthelmintic, analgesic, investigations.
antiviral, anticonvulsant, and CNS-depressant effects.

Table 2 Qualitative Phytochemical analysis of *A. paeoniifolius*

Phytochemical	Test	Ethanol Extract
Alkaloids	Dragendorff's test	++
Flavonoids	Ferric chloride test	+
Terpenoids	Salkowski test	-
Phenols	Lead acetate test	+
Tannins	Ferric chloride test	++
Steroids	Liebermann-Burchard's test	_
Saponins	Frothing test	-
Carbohydrates	Molisch test	+

Presence (+), Absence (-)

GC–MS Analysis of Ethanolic tuber Extract of *A. paeoniifolius*

The GC–MS analysis of the ethanolic tuber extract of *A. paeoniifolius* identified twenty-one phytoconstituents with retention times between 3.07 and 49.12 minutes (**Table 3** and **Fig. 2**), indicating the presence of both volatile and high-molecular-weight compounds. The major constituents included 9,12-octadecadienoic acid (Z, Z) (20.19%), hexadecanoic acid ethyl ester (7.95%), cisvaccenic acid (4.30%), campesterol (5.14%), stigmasterol (8.89%), and ergost-5-en-3-ol (β-sitosterol) (7.06%). These compounds represent key chemical classes such as fatty acids, esters, and phytosterols known for antioxidant, anti-inflammatory, hypolipidemic, and hormonemodulating activities.

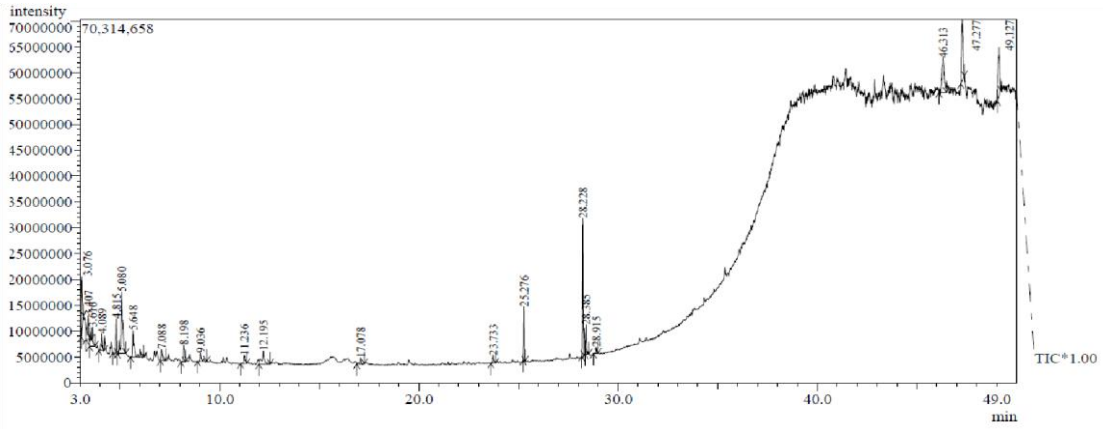

Fig. 2. GC-MS Chromatogram of ethanolic extract of *A. paeoniifolius*

Table 3 Chemical profile of ethanolic tuber extract of *A. paeoniifolius*

Peak No.	RT (min)	% Area 1	% Area 2	Compound Name	Molecular Formula	Molecular Weight (g/mol)
1	3.076	6.33	8.15	Methyl 2-hydroxy-2methylbutyrate	$C_6H_{12}O_3$	132
2	3.407	4.13	3.54	Glycerin	$C_3H_8O_3$	92
3	3.616	4.11	2.78	2-Hexyl acetate	$C_8H_{16}O_2$	144
4	4.089	2.43	2.48	2,5- and 2,6-Dimethyldioxane	$C_6H_{10}O_2$	114
5	4.815	2.52	5.08	3-Methyl-4-methyl-2hexanone	$C_8H_{14}O$	126
6	5.080	11.94	9.00	dl-Glyceraldehyde dimer	$C_6H_{12}O_6$	180
7	5.648	5.32	3.88	1,5-Anhydro-6deoxyhexo-2,3-diulose	$C_6H_8O_4$	144
8	7.088	1.88	1.63	3-Trifluoroacetoxytridecane	$C_{15}H_{27}F_3O_2$	296
9	8.198	2.72	2.49	Phloroglucitol	$C_6H_{12}O_3$	132
10	9.036	1.27	1.26	D-Erythro-2deoxypentose	$C_5H_{10}O_4$	134

11	11.236	1.60	1.25	Lactone G	$C_5H_8O_4$	132
12	12.195	3.59	1.92	trans-7-Pentadecene	$C_{15}H_{30}$	210
13	17.078	0.68	0.89	1-Pentadecene	$C_{15}H_{30}$	210
14	23.733	0.99	1.16	Octadecanal	$C_{18}H_{36}O$	268
15	25.276	4.61	7.95	Ethyl hexadecanoate	$C_{18}H_{36}O_2$	284
16	28.228	12.36	20.19	9,12-Octadecadienoic acid (Z, Z)	$C_{18}H_{32}O_2$	280
17	28.385	2.82	4.30	cis-Vaccenic acid	$C_{18}H_{34}O_2$	282
18	28.915	0.60	0.96	Ethyl octadecanoate	$C_{20}H_{40}O_2$	312
19	46.313	9.70	5.14	Campesterol	$C_{28}H_{48}O$	400
20	47.277	11.04	8.89	Stigmasterol	$C_{29}H_{48}O$	412
21	49.127	9.37	7.06	Ergost-5-en-3-ol (βsitosterol type)	$C_{28}H_{48}O$	400

The (L2) phytosterols identified particularly stigmasterol and βsitosterol are associated with estrogenic and antiandrogenic effects, while linoleic and vaccenic acids support lipid metabolism and insulin sensitivity, suggesting potential relevance in managing PCOS-related metabolic disturbances. The presence of diverse bioactives aligns with previous studies reporting fatty acid derivatives, hydrocarbons, phenolics, and sterols in *A. paeoniifolius* extracts [44, 45]. The higher complexity of the ethanolic extract is consistent with established evidence that solvent extractive values correlate with the abundance of active constituents [46, 47]. Overall, the chemical profile obtained through GC–MS confirms that *A. paeoniifolius* is rich in pharmacologically significant metabolites, supporting its traditional use and potential therapeutic application in PCOS and associated metabolic dysfunctions.

Molecular Docking Analysis

The molecular docking study was performed to predict the binding affinity and interaction profile of the selected bioactive compounds identified from the ethanolic extract of *A. paeoniifolius* with nine PCOS-associated target proteins (PDB IDs: 3FXI, 5F19, and 4X9J). The results are summarized in **Table 4.** Among the phytocompounds analyzed, 9,12-octadecadienoic acid exhibited the strongest binding affinity, with docking scores of −6.0 kcal/mol (3FXI), −5.6 kcal/mol (5F19), and −6.0 kcal/mol (4X9J). These values indicate stable interactions with all three PCOS-related targets. cis-Vaccenic acid (L3) also demonstrated notable binding affinity, particularly against 3FXI (−5.9 kcal/mol) and 5F19 (−5.7 kcal/mol). Importantly, the binding affinity of cis-Vaccenic acid toward these two targets was comparable to or slightly higher than that of the standard drug Metformin (D1), which showed docking scores of −5.2 kcal/mol (3FXI) and −5.5 kcal/mol (5F19). However, against 4X9J, cisVaccenic acid exhibited lower binding affinity (−4.8 kcal/mol) compared to Metformin (−5.5 kcal/mol), suggesting target-specific interaction variability.

Table 4 Molecular docking results of *A. paeoniifolius* phytocompounds and standard drugs with PCOS-associated target proteins

Ligands	Ligand code	Bonding enrgy (kcal/mol)		
		3FXI	5F19	4X9J
Lactone G	L1	-4.4	-4.4	-4.3
9,12-Octadecadienoic acid	L2	-6.0	-5.6	-6.0
cis-Vaccenic acid	L3	-5.9	-5.7	-4.8
Metformin	D1	-5.2	-5.5	-5.5

The molecular docking analysis of phytoconstituents identified in the ethanolic tuber extract of *A. paeoniifolius* revealed strong and stable interactions with all three selected receptor proteins, indicating their potential biological relevance in the management of PCOS. The standard drug Metformin (D1) displayed moderate and consistent binding across all three targets, confirming its established role in PCOS management. In contrast, Lactone G (L1) showed the weakest interactions, with binding energies ranging from −4.3 to −4.4 kcal/mol, indicating limited binding potential. Collectively, the docking results suggest that cis-Vaccenic acid and 9,12octadecadienoic acid exhibit promising binding affinities comparable to the standard drug Metformin, highlighting their potential as bioactive phytocompounds for further investigation in PCOS-related therapeutic studies.

ligands Lactone G (γ-butyrolactone, L1), linoleic acid (L2), and cis-vaccenic acid (L3) displayed multiple binding contacts including hydrogen bonds and hydrophobic interactions within the active pockets of the target proteins.

The standard reference ligand, Metformin (D1), exhibited both types of interactions, as outlined in **Table 5.**

Table 5 Interaction of aminoacid residues with ligands at receptor sites

Protein	Ligands	Amino acids involved and distance (Å)	
		Hydrogen-Binding Interaction	Hydrophobic Interaction
3FXI	L1	127C Ser (2.69), 441B Ser (2.86)	82C Val (3.70), 126C Phe (3.61), 131C Tyr (3.74)
	L2	_____	32C Ile (3.63, 3.73), 52C Ile (3.44), 61C Leu (3.72, 3.76), 63C Ile (3.92), 76C Phe (3.78), 119C Phe (3.87, 3.47), 147C Phe (3.74), 149C Leu (3.61), 151C Phe (3.75, 3.75, 3.63)
	L3	125D Lys (2.47), 127D Ser (2.67), 417A Asn (3.16), 441A Ser (2.23)	54D Leu (3.57), 80D Ile (3.54), 82D Val (3.49), 121D Phe (3.39, 3.51), 126D Phe (3.90, 3.41), 440A Phe (3.62)
	D1	292A Tyr (2.59, 3.24), 296A Tyr (3.10), 317A Ser (2.89), 319A Thr (2.62)	_____
5F19	L1	385A Tyr (2.09), 526A Gly (2.02), 533A Gly (2.77), 534A Leu (2.46)	205A Phe (3.87), 344A Val (3.49), 348A Tyr (3.91)
	L2	385A Tyr (2.09), 526A Gly (2.02), 533A Gly (2.77), 534A Leu (2.46)	205A Phe (3.87), 344A Val (3.49), 348A Tyr (3.91)
	L3	385A Tyr (2.09), 526A Gly (2.02), 533A Gly (2.77), 534A Leu (2.46)	205A Phe (3.87), 344A Val (3.49), 348A Tyr (3.91)
	D1	385A Tyr (2.09), 526A Gly (2.02), 533A Gly (2.77), 534A Leu (2.46)	205A Phe (3.87), 344A Val (3.49), 348A Tyr (3.91)
4X9J	L1	_____	226A His (3.82), 248A Tyr (3.45)
	L2	248A Tyr (2.25)	188A Leu (3.56, 3.65), 222A Leu (3.83, 3.42), 223A Val (3.43), 226A His (3.71), 243A Leu (3.34), 248A Tyr (3.59), 251A Thr (3.99), 255A Pro (3.83)
	L3	245A Tyr (2.60)	188A Leu (3.88), 218A Tyr (3.71), 223A Val (3.55), 226A His (3.77)
	D1	222A Leu (2.81), 243A Leu (2.14), 249A Arg (2.46)	_____

For the 3FXI protein, L1 formed hydrogen bonds with Ser127C and Ser441B, complemented by hydrophobic contacts with Val82C, Phe126C, and Tyr131C. L2 exhibited extensive hydrophobic interactions with Ile32C, Ile52C, Leu61C, Phe76C, and Phe151C, while L3 showed additional hydrogen bonding with Lys125D, Ser127D, Asn417A, and Ser441A. These interactions were comparable to or stronger than those observed with standard drugs, where metformin (D1) engaged residues such as Tyr292A, Tyr296A, Ser317A, and Thr319A (**Fig. 3 to 6**).

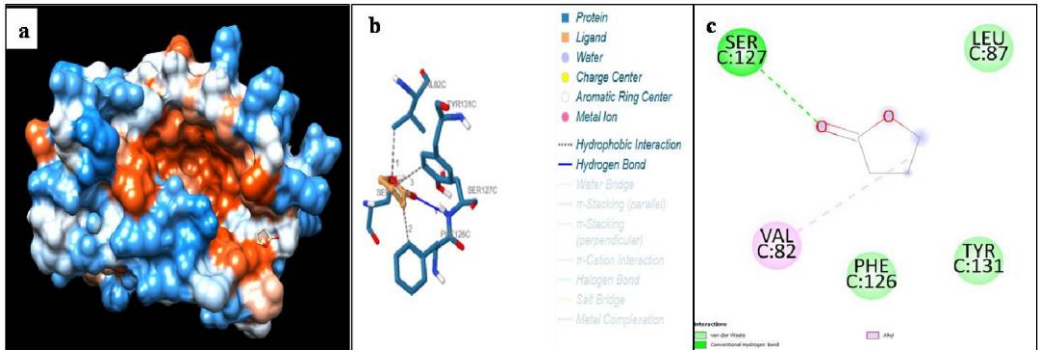

*Author for Correspondence: sailakedaram@gmail.com

Fig. 3. Surface model of PDB: 3FXI showing L1 (Lactone G) molecular interactions (a), molecular binding (b), and target protein (c)

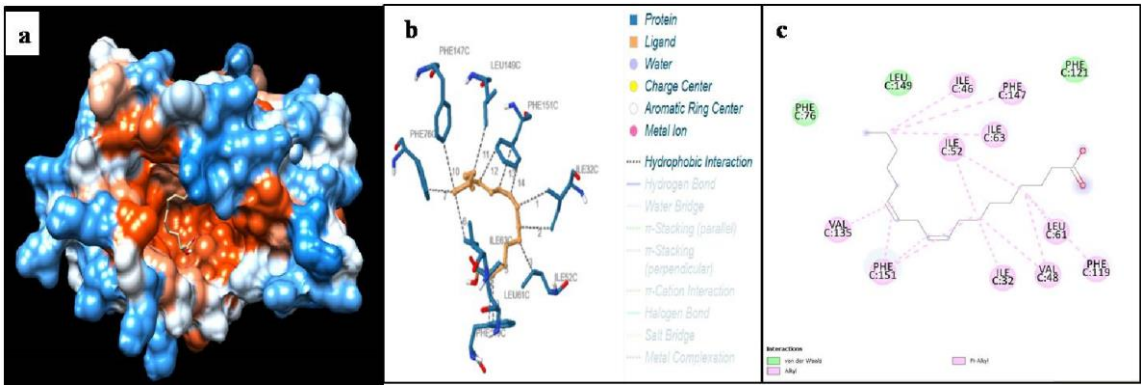

Fig. 4. Surface model of PDB: 3FXI showing L1 (9,12-octadecadienoic acid) molecular interactions (a), molecular binding (b), and target protein (c)

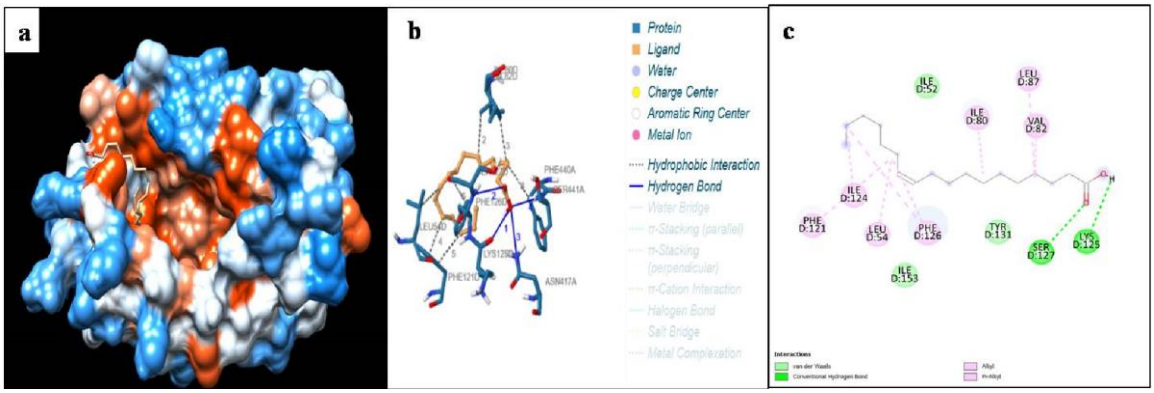

Fig. 5. Surface model of PDB: 3FXI showing L1 (cis-vaccenic acid) molecular interactions (a), molecular binding (b) and target protein (c)

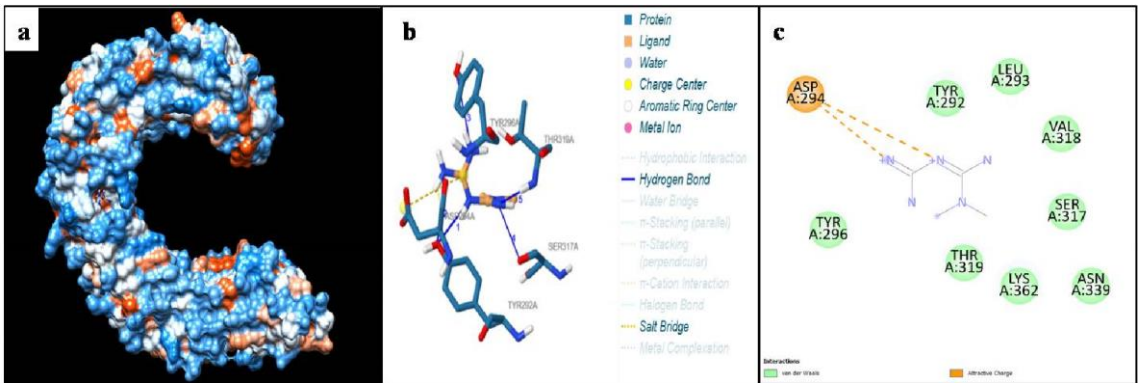

Fig. 6. Surface model of PDB: 3FXI showing D1 (Metformin) molecular interactions (a), molecular binding (b), and target protein (c)

A similar interaction pattern was observed for the 5F19 hydrophobic interactions with Phe205A, Val344A, and protein. All three phytocompounds (L1–L3) and the Tyr348A, suggesting that these residues represent a key standard drugs formed conserved hydrogen bonds with recognition motif across structurally diverse ligands (**Fig.** Tyr385A, Gly526A, Gly533A, and Leu534A, and **7** **to** **10**).

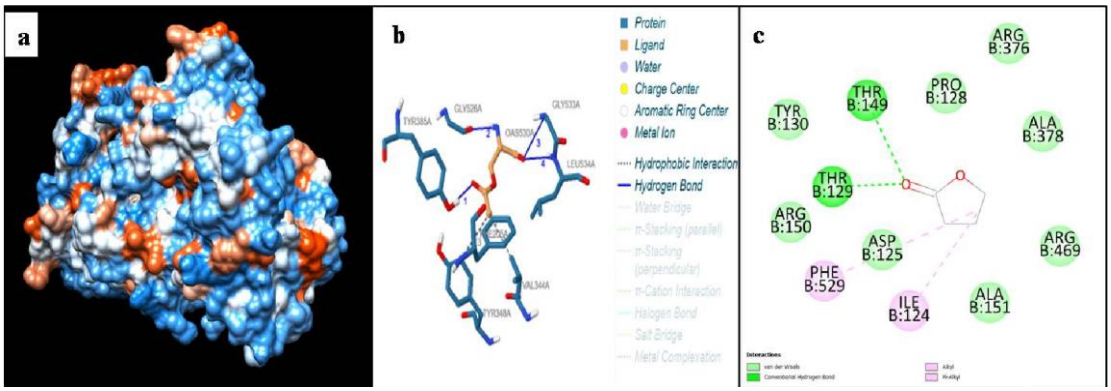

Fig. 7. Surface model of PDB: 3F19 showing L1 (Lactone) molecular interactions (a), molecular binding (b), and target protein (c)

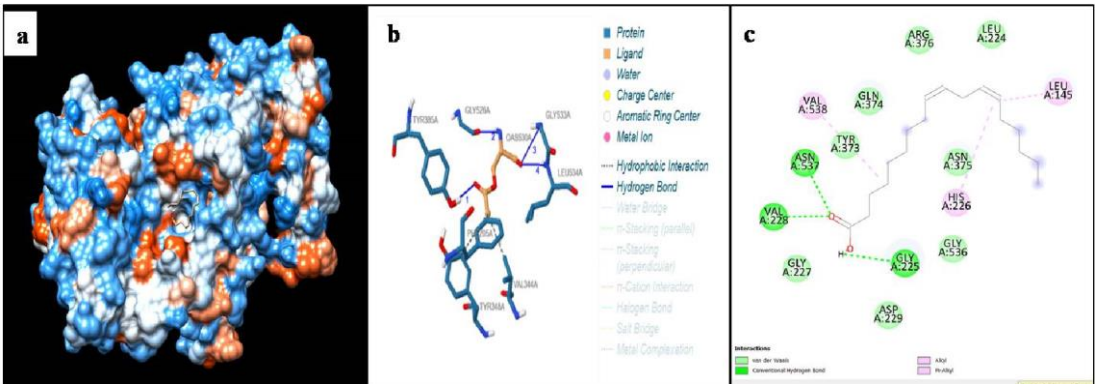

Fig. 8. Surface model of PDB: 3F19 showing L2 (9,12-octadecadienoic acid) molecular interactions (a), molecular binding (b) and target protein (c)

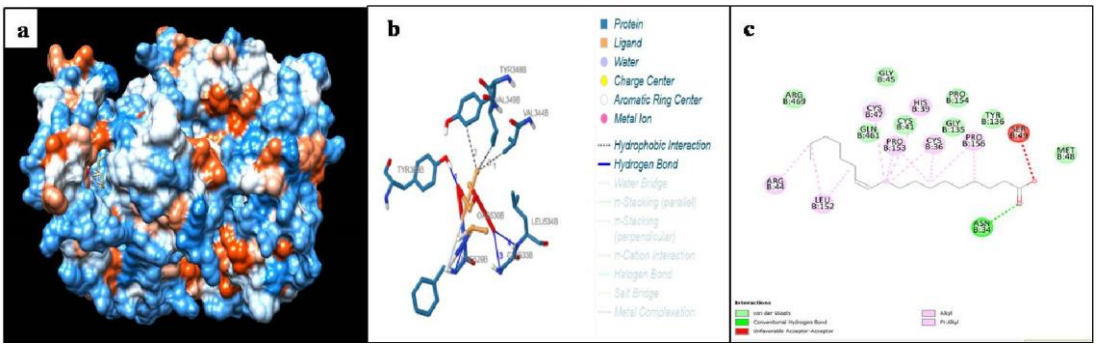

Fig. 9. Surface model of PDB: 3F19 showing L3 (cis-vaccenic acid) molecular interactions (a), molecular binding (b), and target protein (c)

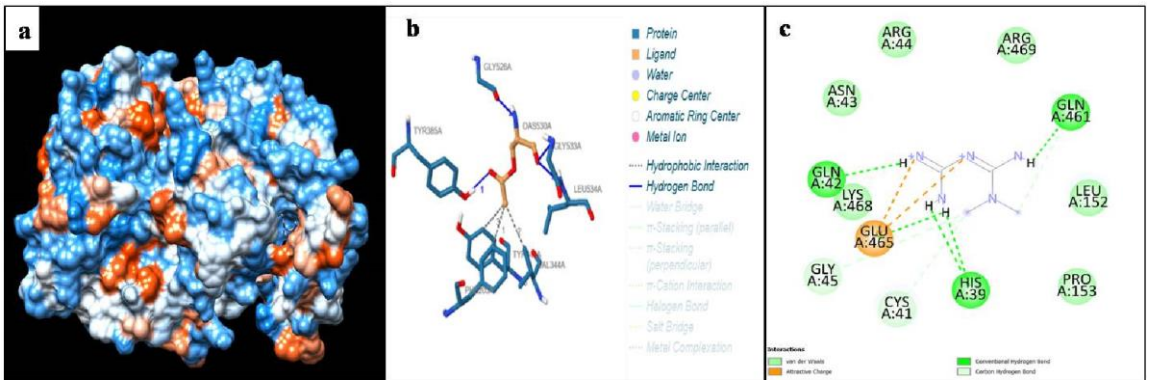

Fig. 10. Surface model of PDB: 3F19 showing D1 (Metformin) molecular interactions (a), molecular binding (b), and target protein (c)

In the 4X9J protein, L1 primarily engaged in hydrophobic interactions with His226A and Tyr248A. L2 formed a strong hydrogen bond with Tyr248A along with hydrophobic contacts involving Leu188A, Leu222A, Val223A, and Pro255A. L3 exhibited hydrogen bonding with Tyr245A and additional hydrophobic interactions with Leu188A, Tyr218A, and His226A. Metformin and clomiphene citrate also interacted with essential catalytic residues, but the phytocompounds demonstrated comparable, and in some cases superior, affinity and interaction stability. Collectively, these findings highlight the consistent binding performance of L1, L2, and L3 across all receptor sites, supporting their potential as bioactive leads for PCOS management (**Fig. 11 to 14**).

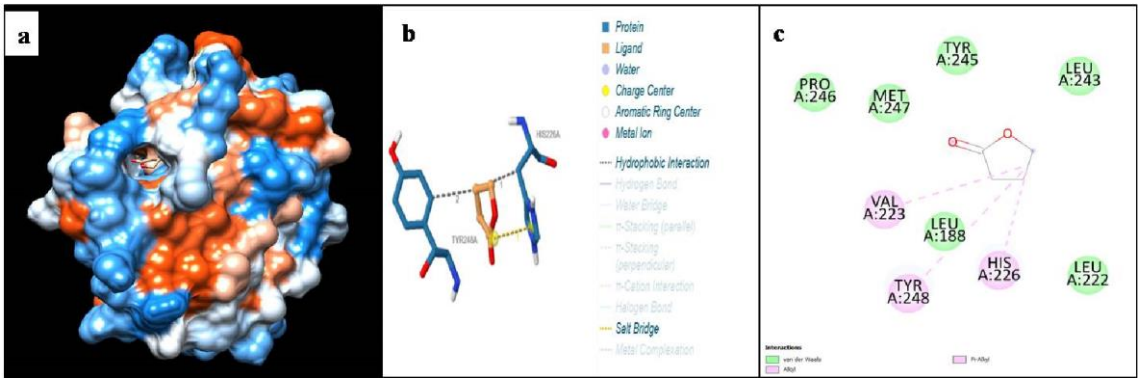

Fig. 11. Surface model of PDB: 4X9J showing L1 (Lactone) molecular interactions (a), molecular binding (b) and target protein (c)

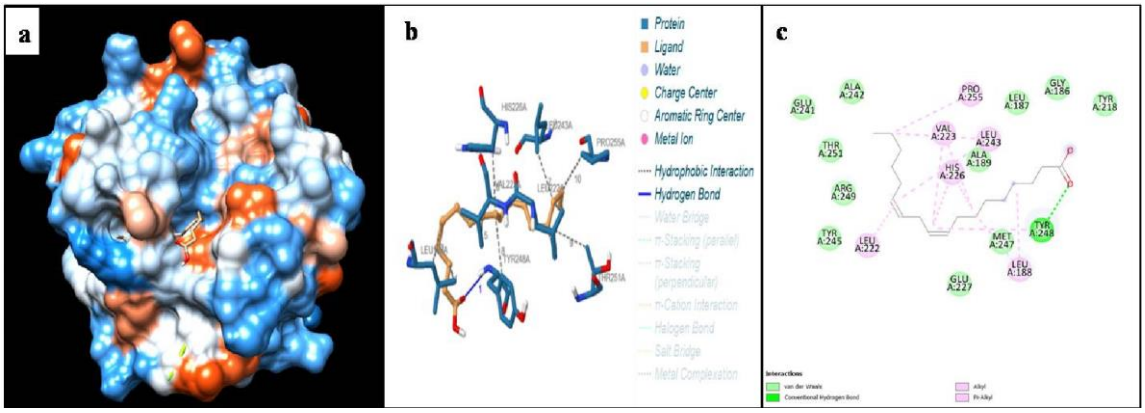

Fig. 12. Surface model of PDB: 4X9J showing L2 (9,12-octadecadienoic acid) molecular interactions (a), molecular binding (b), and target protein (c)

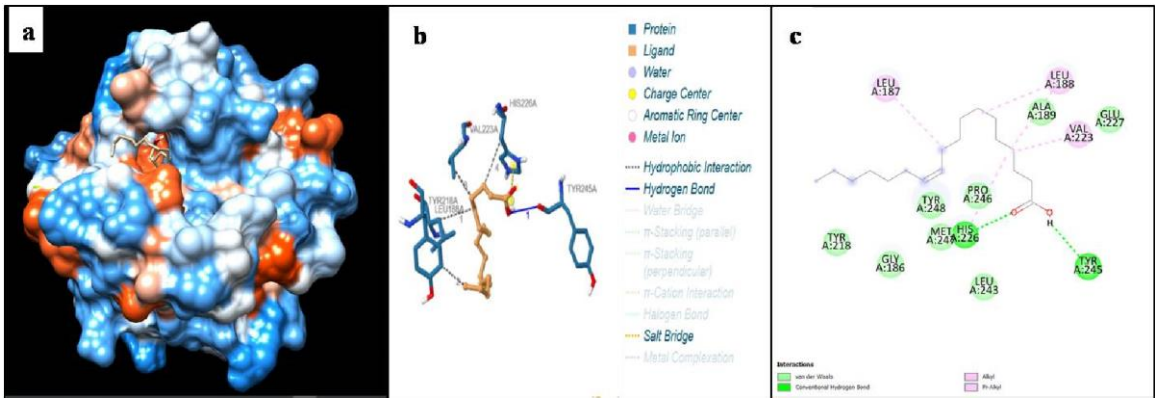

Fig. 13. Surface model of PDB: 4X9J showing L2 (cis-vaccenic acid) molecular interactions (a), molecular binding (b), and target protein (c)

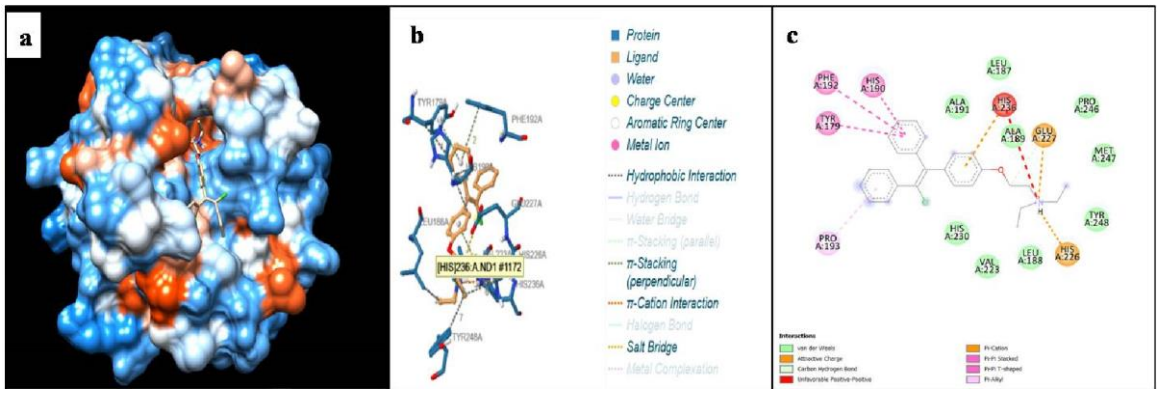

Fig. 14. Surface model of PDB: 4X9J showing D1 (Metformin) molecular interactions (a), molecular binding (b) and target protein (c)

The docking results align with growing evidence supporting the therapeutic contribution of plant-derived compounds in PCOS. A recent review documented that various phytoconstituents such as Rumphioside I, anethole, quercetin, naringenin, carvone, rutin, and kaempferol show significant affinity for PCOS-related targets including IRS1, IRS2, 3RUK, 1E3G, and 1XUN [48]. Similarly, cis-vaccenic acid and octadecanoic acid have demonstrated strong binding affinity toward CYP19A1 and AdipoR1, with docking scores of −6.4 and −7.6 kcal/mol, respectively, indicating their relevance in inflammatory and metabolic signaling in PCOS. In another study, a sugar-derived lactone showed more favorable binding scores than metformin across four metabolic enzymes linked to PCOS [49],

supporting the functional significance of the lactone scaffold, consistent with the strong binding behavior observed for L1 in the present study.

Among the phytocompounds analyzed, Lactone G (L1) displayed particularly strong affinity for steroidogenic and metabolic receptors. Lactone-based molecules have been previously characterized as multifunctional regulators of oxidative stress, metabolic enzymes, and neuroendocrine pathways [50]. Prior studies also reported that lactone derivatives exhibit stronger inhibitory activity than metformin on enzymes such as PEPCK, α-amylase, βglucosidase, and fructose-1,6-bisphosphatase [51], reinforcing the relevance of the lactone backbone. Linoleic acid (L2) also demonstrated robust docking interactions with PCOS-related proteins. Recent experimental evidence confirms that linoleic acid directly binds the estrogen receptor (ERα), activating FOXO1, ROS, and NF-κB signaling pathways in granulosa cells [52]. Although this activation contributes to cellular stress *in vitro*, the findings establish linoleic acid as an ER-binding ligand. Docking and network-pharmacology studies have also predicted linoleic acid derivatives to modulate PPARG, a central regulator of insulin sensitivity in PCOS [53] , supporting the mechanistic plausibility of its interactions observed in the present analysis. cis-Vaccenic acid (L3), although comparatively understudied in PCOS, is structurally aligned with monounsaturated fatty acids (MUFAs), which modulate inflammation, lipid signaling, and glucose homeostasis pathways commonly altered in PCOS [54].

Its strong binding interactions across all protein targets analyzed suggest that MUFAs may act as modulators of endocrine–metabolic pathways relevant to PCOS pathophysiology.

ADMET Profiling and Drug-Likeness Prediction

The ADMET and drug-likeness assessment of Lactone G (L1), 9,12-octadecadienoic acid (Z, Z) (L2), and cisvaccenic acid (L3) was performed to evaluate their pharmacokinetic suitability as oral drug candidates (**Table 6**). All three compounds exhibited molecular weights between 86.09 and 282.46 g/mol, well below the 500 g/mol threshold recommended for favorable oral bioavailability. Their hydrogen bond donor and acceptor count also fell within the limits of Lipinski's Rule of Five, except for L3, which showed a single violation due to elevated lipophilicity (LogP = 5.7). Although high lipophilicity may occasionally hinder aqueous solubility, it can simultaneously facilitate membrane permeability and passive absorption, especially for lipid-derived molecules.

Lactone G (L1), the smallest phytocompound ($C_4H_6O_2$; 86.09 g/mol), displayed optimal physicochemical features with low lipophilicity (consensus LogP = 0.47), high predicted solubility, and excellent gastrointestinal (GI) absorption. Importantly, L1 showed no blood–brain barrier (BBB) permeability and was not identified as a substrate for P-glycoprotein (P-gp), minimizing the likelihood of efflux-mediated loss. Its bioavailability score of 0.55 further suggests efficient systemic circulation following oral administration.

Linoleic acid (L2) exhibited moderate lipophilicity (LogP near zero), two hydrogen-bond acceptors, and one donor, consistent with good physicochemical balance. Although its solubility was relatively lower than L1, its high molar refractivity (89.46) reflects strong van der Waals interaction capacity, favoring receptor binding. L2 also lacked BBB permeability and P-gp interactions, supporting its known safety and biocompatibility characteristics. However, its polyunsaturated nature may compromise stability, as such fatty acids are more vulnerable to oxidative degradation.

cis-Vaccenic acid (L3) demonstrated the most favorable ADMET profile among the evaluated compounds. Its moderate topological polar surface area (TPSA = 20.23 Å^2), high lipophilicity (LogP = 5.7), and excellent bioavailability score (0.85) collectively indicate strong permeability and good oral absorption. L3 showed no BBB permeability and no predicted interactions with P-gp, which is advantageous for minimizing CNS side effects and avoiding drug efflux. Its elevated molar refractivity (89.94) and high fraction of sp^3 carbons (0.83) further support molecular flexibility and stable biological interactions.

The BOILED-Egg predictive model (**Fig. 15**), generated using SwissADME, corroborated these findings. This model estimates passive absorption and BBB penetration based on WLogP and TPSA [55]. L3 was positioned within the "white" region indicating high probability of intestinal absorption yet remained outside the "yolk" region, confirming low BBB permeation. L1 also fell within the optimal absorption zone, whereas L2 appeared near the boundary between high and low absorption areas, consistent with its intermediate physicochemical properties. As reported by Pandey *et al*. [56], molecules located in the white region of the BOILED-Egg graph typically display good oral availability, low toxicity, and favorable permeability profiles.

Recent phytochemical screenings for PCOS therapeutics often prioritize flavonoids, alkaloids, and terpenoids because they meet classical drug-likeness filters, leading to fewer evaluations of long-chain fatty acids such as linoleic or vaccenic acid [57]. This underrepresentation is a methodological bias rather than a true reflection of weak pharmacological potential, emphasizing the importance of comprehensive ADMET-based evaluations like the present study.

Overall, cis-vaccenic acid (L3) emerged as the most pharmacokinetically robust compound. Its combination of high lipophilicity, optimal TPSA, strong GI absorption, and high predicted bioavailability supports its potential as an orally active therapeutic candidate. The monounsaturated structure of L3 enhances membrane permeability and confers greater oxidative stability than polyunsaturated fatty acids like L2, which produce proinflammatory

TPSA	37.3	36.68	20.23
Fraction Csp3	0.75	0.72	0.83
Rotatable bonds	0	14	15
LogP (Consensus)	0.47	0	5.7
Solubility (ESOL)	Highly solubility	Low	Moderately soluble
GI absorption	High	-	High
BBB permeant	NO	NO	NO
Rule of 5	0	-	1
Bioavailability Score	0.55	-	0.85

metabolites and oxidative byproducts in granulosa cells [52]. Metabolically, MUFAs such as cisvaccenic acid undergo predictable β-oxidation, show low CYP450 inhibition risk, and generate no harmful intermediates [58].

This is advantageous compared with L2, which is known to generate reactive lipid species that adversely affect ovarian physiology.

In contrast, although γ-butyrolactone (L1) exhibited excellent solubility and GI absorption due to its small polar structure, its lower lipophilicity may limit stable interaction with lipid-rich biological targets. cis-Vaccenic acid (L3), with its balanced hydrophobicity and structural stability, demonstrated superior overall ADMET characteristics, positioning it as a promising lead molecule for further preclinical validation and pharmacodynamic studies in PCOS.

The *in-silico* toxicity assessment (**Table 7** and **Fig. 16**) demonstrated that all three ligands (L1–L3) exhibited a favorable safety profile, showing no carcinogenic, mutagenic, hepatotoxic, or cytotoxic potential, and remained largely inactive across key toxicological endpoints. None of the compounds showed predicted neurotoxicity, nephrotoxicity, or cardiotoxicity, indicating a wide preliminary safety margin. Among them, L3 showed predicted activation of PPAR-γ, Nrf2/ARE, and HSE pathways, suggesting its possible involvement in antioxidant defense, metabolic regulation, and cellular stress adaptation mechanisms that are beneficial in PCOSassociated oxidative and inflammatory conditions [59, 60, 54].

L2 and L3 presented mild ecotoxic potential (probability ≈ 0.65), while L1 showed moderate binding to transthyretin (TTR), though without major toxicity implications. LD_{50} estimates revealed substantial variability, classifying L2 (10,000 mg/kg) as non-toxic (class 6), L1 (1,460 mg/kg) as slightly toxic (class 4), and L3 (48 mg/kg) as toxic (class 2); however, the absence of predicted interactions with major cytochrome P450 isoforms across all compounds suggests minimal risk of metabolic interference or drug–drug interactions (Hines, 2008). Overall, the toxicity profiling supports the pharmacological safety of L1 and L2, while L3, despite its biological potency, requires cautious dose optimization. The mild ecotoxicity predicted for L2 and L3 reflects environmental considerations rather than human toxicity [61].

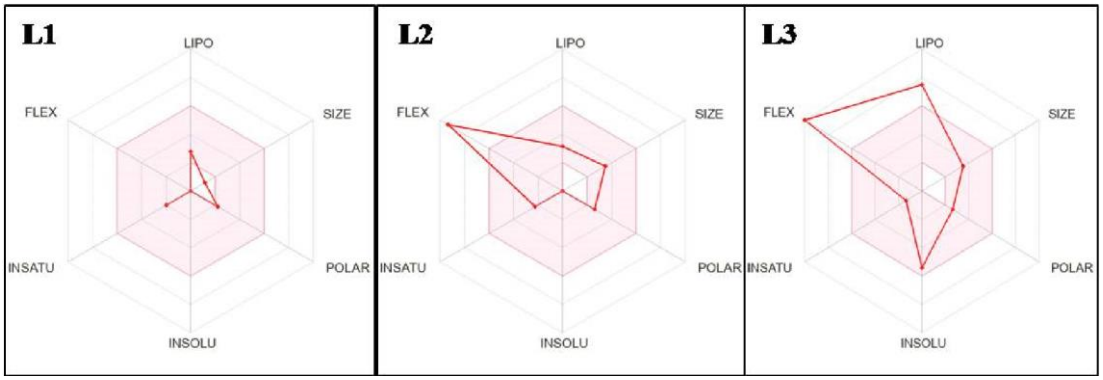

Fig. 15. Boiled Egg plot of WlogP versus TPSA for L1, L2, and L3, highlighting L3 within the optimal range for favorable pharmacokinetic and therapeutic potential.

Table 6 Phytochemical and pharmacokinetic properties of screened compounds (ADMETprofiling - L1 to L3)

Toxicity Profiling and Safety Evaluation

Ligand code	**L1**	**L2**	**L3**
Molecular formula	$C_4H_6O_2$	$C_{18}H_{32}O_2$	$C_{18}H_{34}O_2$
Smile ID	O=C1CCCO1	CCCCC/C=C\C/C=C\CCCCC CCC(=O)O	CCCCCC/C=C\CCCC CCCCCC(=O)O
Molecular weight	86.09g/mol	280.45g/mol	282.46g/mol
HB acceptor	2	2	2
HB donor	0	IJDDT, Volume 16 Issue 3, 2026	1
iLOGP	1.13	0	4.25
Molar refractivity	20.51	89.46	89.94

Table 7 Predicted toxicity profiles of selected compounds (L1–L3) and predicted LD_{50} values with corresponding toxicity classes

Property	Prediction (Probability)		
Toxicity Prediction	**L1**	**L2**	**L3**
Hepatotoxicity	Inactive (0.73)	Inactive (0.55)	Inactive (0.55)
Neurotoxicity	Inactive (0.64)	Inactive (0.91)	Inactive (0.91)
Nephrotoxicity	Inactive (0.52)	Inactive (0.55)	Inactive (0.55)
Respiratory Toxicity	Inactive (0.96)	Inactive (0.84)	Inactive (0.84)
Cardiotoxicity	Inactive (0.74)	Inactive (0.99)	Inactive (0.99)
Carcinogenicity	Inactive (0.76)	Inactive (0.64)	Inactive (0.64)
Immunotoxicity	Inactive (0.99)	Inactive (0.96)	Inactive (0.99)
Mutagenicity	Inactive (0.96)	Inactive (1.0)	Inactive (1.0)
Cytotoxicity	Inactive (0.70)	Inactive (0.71)	Inactive (0.71)
BBB Barrier	Active (0.91)	Active (0.89)	Active (0.89)
Ecotoxicity	Active (0.53)	Active (0.65)	Active (0.65)
Clinical Toxicity	Inactive (0.64)	Inactive (0.61)	Inactive (0.61)
Nutritional Toxicity	Inactive (0.81)	Inactive (0.89)	Inactive (0.89)
Aryl Hydrocarbon Receptor (AhR)	Inactive (0.99)	Inactive (1.0)	Inactive (1.0)
Androgen Receptor (AR)	Inactive (0.99)	Inactive (1.0)	Inactive (1.0)
Androgen Receptor Ligand Binding Domain (AR-LBD)	Inactive (0.99)	Inactive (1.0)	Inactive (1.0)
Aromatase	Inactive (1.0)	Inactive (1.0)	Inactive (1.0)
Estrogen Receptor Alpha (ER)	Inactive (0.99)	Inactive (1.0)	Inactive (1.0)
Estrogen Receptor Ligand Binding Domain (ER-LBD)	Inactive (0.99)	Inactive (1.0)	Inactive (1.0)
Peroxisome Proliferator Activated Receptor Gamma (PPAR-γ)	Inactive (0.99)	Active (0.90)	Active (0.90)
Nrf2/ARE Pathway	Inactive (1.0)	Active (0.91)	Active (0.91)
Heat Shock Factor Response Element (HSE)	Inactive (1.0)	Active (0.91)	Active (0.91)
Mitochondrial Membrane Potential (MMP)	Inactive (1.0)	Inactive (1.0)	Inactive (1.0)
Phosphoprotein (Tumor Suppressor) p53	Inactive (0.99)	Inactive (1.0)	Inactive (1.0)
ATPase Family AAA Domaincontaining Protein 5 (ATAD5)	Inactive (0.99)	Inactive (1.0)	Inactive (1.0)
Thyroid Hormone Receptor Alpha (THRα)	Inactive (0.78)	Inactive (0.90)	Inactive (0.73)
Thyroid Hormone Receptor Beta (THRβ)	Inactive (0.88)	Inactive (0.78)	Inactive (0.91)
Transthyretin (TTR)	Active (0.58)	Inactive (0.97)	Inactive (0.74)
Ryanodine Receptor (RYR)	Inactive (0.94)	Inactive (0.98)	Inactive (0.96)
GABA Receptor (GABAR)	Inactive (0.58)	Inactive (0.96)	Inactive (0.56)
Glutamate NMDA Receptor (NMDAR)	Inactive (0.93)	Inactive (0.92)	Inactive (0.98)
AMPA Receptor (AMPAR)	Inactive (0.99)	Inactive (0.97)	Inactive (1.0)
Kainate Receptor (KAR)	Inactive (1.0)	Inactive (0.99)	Inactive (1.0)
Acetylcholinesterase (AChE)	Inactive (0.77)	Inactive (0.55)	Inactive (0.68)

Constitutive Androstane Receptor (CAR)	Inactive (0.99)	Inactive (0.98)	Inactive (0.99)
Pregnane X Receptor (PXR)	Inactive (0.55)	Inactive (0.92)	Active (0.59)
NADH-Quinone Oxidoreductase (NADHOX)	Inactive (0.51)	Inactive (0.97)	Active (0.59)
Voltage-Gated Sodium Channel (VGSC)	Inactive (0.88)	Inactive (0.95)	Inactive (0.93)
Na+/I− Symporter (NIS)	Inactive (0.82)	Inactive (0.98)	Inactive (0.93)
Cytochrome CYP1A2	Inactive (0.80)	Inactive (0.91)	Inactive (0.91)
Cytochrome CYP2C19	Inactive (0.86)	Inactive (0.98)	Inactive (0.98)
Cytochrome CYP2C9	Inactive (0.63)	Inactive (0.69)	Inactive (0.69)
Cytochrome CYP2D6	Inactive (0.81)	Inactive (0.88)	Inactive (0.88)
Cytochrome CYP3A4	Inactive (0.96)	Inactive (1.0)	Inactive (1.0)
Cytochrome CYP2E1	Inactive (0.94)	Inactive (0.99)	Inactive (0.99)
Predicted LD50 (mg/kg)	1460 mg/kg	10000 mg/kg	48 mg/kg
Predicted Toxicity Class	4	6	2

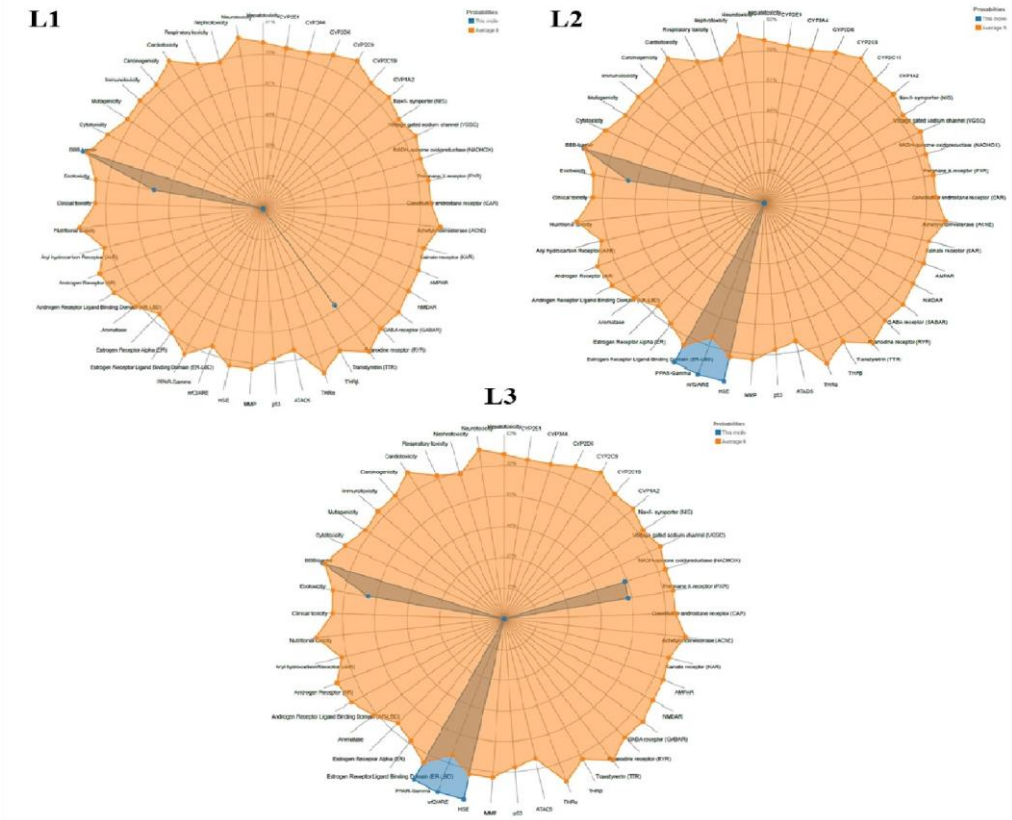

Fig. 16. Radar chart of toxicities of phytocompound L1, L2, L3, L4, L5, L6 and drug by PROTOX

***In silico* PASS Prediction Study**

The PASS prediction analysis (**Table 8**) revealed that all three ligands exhibited a broad spectrum of biological activities with high confidence levels (Pa > 0.5), indicating strong pharmacological potential. Lactone G (L1) showed predicted antineoplastic, antimetastatic, and anti-infective activities, suggesting possible anticancer and antimicrobial utility consistent with earlier reports that lactone derivatives possess notable cytotoxic and antimicrobial effects [50, 62]. Linoleic acid (L2) demonstrated pronounced antimutagenic, antihypercholesterolemic, antithrombotic, and anti-inflammatory properties, in accordance with established evidence describing the role of polyunsaturated fatty acids in modulating lipid metabolism, reducing inflammation, and improving cardiovascular health [63, 64]. Notably, cis-vaccenic acid (L3) displayed the highest Pa value (0.956) as an acylcarnitine hydrolase inhibitor, alongside antimutagenic, antiviral, and antidiabetic potential, highlighting its relevance in metabolic dysfunctions such as insulin resistance and dyslipidemia as well as in infectious diseases. These predictions are aligned with growing evidence demonstrating that monounsaturated fatty acids contribute to enhanced insulin sensitivity and antiviral response modulation [54, 65].

Collectively, the PASS results underline the multifunctional therapeutic relevance of these phytochemicals, with cis-vaccenic acid emerging as the strongest candidate due to its wide-ranging and high-confidence predicted activities, thereby providing a compelling basis for further experimental validation in metabolic, inflammatory, and infectious disease models.

Table 8 biological activity of Lactone, 9,12-octadecadienoic acid and cis-vaccenic acid by using *in silico* pass prediction study

Compound	Pa	Pi	Predicted Biological Activity
Lactone G (L1)	0.756	0.018	Antineoplastic
	0.664	0.044	Antiseborrheic
	0.628	0.032	Antidyskinetic
	0.571	0.022	Antihypoxic
	0.549	0.011	Antimetastatic
	0.538	0.019	Antiinfective
	0.497	0.052	Antiviral (Picornavirus)
	0.484	0.027	Antiprotozoal (Leishmania)
	0.481	0.019	Antihelmintic (Nematodes)
	0.454	0.026	Antimyopathies

CONCLUSION

The present study demonstrates that the ethanolic tuber extract of *A. paeoniifolius* contains multiple bioactive compounds, including linoleic acid and cis-vaccenic acid, with significant pharmacological potential. Molecular docking studies revealed strong and energetically favorable interactions of these compounds with multiple PCOS-associated target proteins, comparable to standard drugs such as metformin and clomiphene citrate. ADMET and toxicity profiling indicated favorable pharmacokinetic properties and safety, with cis-vaccenic acid showing optimal oral bioavailability and minimal metabolic liabilities. PASS prediction further highlighted multifunctional therapeutic potential, particularly antidiabetic, antiviral, and antimutagenic activities for cisvaccenic acid. Collectively, these findings identify cisvaccenic acid as a promising lead compound for further development as a therapeutic agent targeting PCOS and related metabolic dysfunctions. The study provides a strong rationale for subsequent *in vitro* and *in vivo* validation to confirm efficacy and safety, potentially contributing to the discovery of novel plant-based interventions for PCOS.

	0.443	0.017	Antineoplastic (Colorectal cancer)
	0.435	0.017	Antineoplastic (Colon cancer)
	0.426	0.020	Antineoplastic (Lung cancer)
9,12-Octadecadienoic acid (L2)	0.792	0.004	Antimutagenic
	0.774	0.005	Antihypercholesterolemic
	0.732	0.006	Antithrombotic
	0.730	0.012	Antiinflammatory
	0.701	0.008	Antihypoxic
	0.658	0.007	Antiulcerative
	0.597	0.020	Antiviral (Picornavirus)
	0.536	0.018	Antipsoriatic
	0.438	0.025	Anticarcinogenic
	0.435	0.076	Antineoplastic (Non-Hodgkin's lymphoma)
	0.424	0.025	Antituberculosic
	0.400	0.049	Antiprotozoal (Leishmania)
cis-Vaccenic acid (L3)	0.956	0.002	Acylcarnitine hydrolase inhibitor
	0.852	0.003	Antimutagenic
	0.685	0.003	Antiinflammatory (Intestinal)
	0.693	0.011	Kidney function stimulant
	0.665	0.009	Antiinfective
	0.652	0.009	Antiviral (Influenza)
	0.649	0.006	Antipruritic (Allergic)
	0.635	0.008	Antiulcerative
	0.558	0.002	Antiviral (CMV)
	0.532	0.018	Antipsoriatic
	0.498	0.031	Antifungal
	0.449	0.017	Antiseptic
	0.439	0.023	Antiparasitic
	0.425	0.014	Antihelmintic
	0.416	0.012	Antidiabetic symptomatic
	0.415	0.028	Anticarcinogenic
	0.407	0.029	Antituberculosic

Funding Statement There is no funding

Data Availability Statement
The data presented in this study are available upon request from the first author.

Declaration
Competing Interest, the authors declare that they have no known competing financial interests or personal relationships that could have appeared to influence the work reported in this paper. This study did not involve any experiments on human participants or animals conducted by the authors

REFERENCES

1. Escobar-Morreale, H. F. (2018). *Polycystic ovary syndrome: Definition, aetiology, diagnosis and treatment.* Nature Reviews Endocrinology, 14(5), 270–284. DOI: 10.1038/nrendo.2018.24
2. Lizneva, Daria; Suturina, Larisa; Walker, Walidah; Brakta, Soumia; Gavrilova-Jordan, Larisa; Azziz, Ricardo. (2016). *Criteria, prevalence, and phenotypes of polycystic ovary syndrome.* Fertility and Sterility, 106(1), 6–15. DOI: 10.1016/j.fertnstert.2016.05.003
3. Goodarzi, M. O.; Dumesic, D. A.; Chazenbalk, G.; Azziz, R. (2011). *Polycystic ovary syndrome: Etiology, pathogenesis and diagnosis.* Nature Reviews Endocrinology, 7(4), 219–231. DOI: 10.1038/nrendo.2010.217
4. Dumesic, D. A.; Oberfield, S. E.; Stener-Victorin, E.; Marshall, J. C.; Laven, J. S.; Legro, R. S. (2015). *Scientific statement on the diagnostic criteria, epidemiology, pathophysiology, and molecular genetics of polycystic ovary syndrome.* Endocrine Reviews, 36(5), 487–525. DOI: 10.1210/er.2015-1018
5. Azziz, R. (2016). *Polycystic ovary syndrome.* Obstetrics & Gynecology, 127(5), 913–927.

6. Witchel, Selma F.; Oberfield, Sharon E.; Peña, Alexia S. (2019). *Polycystic ovary syndrome: pathophysiology, presentation, and treatment with emphasis on adolescent girls.* Journal of the Endocrine Society, 3(8), 1545–1573. DOI: 10.1210/js.2019-00078

7. González, Frank; Sia, Chang-Ling; Shepard, Marguerite K.; Rote, Neal S.; Minium, Judi. (2012). *Hyperglycemia-induced oxidative stress is independent of excess abdominal adiposity in normal-weight women with polycystic ovary syndrome.* Human Reproduction, 27(12), 3560–3568. DOI: 10.1093/humrep/des320

8. Franks, Stephen; Hardy, Kate. (2018). *Androgen action in the ovary.* Frontiers in Endocrinology, 9, 452. DOI: 10.3389/fendo.2018.00452

9. Rosenfield, Robert L.; Ehrmann, David A. (2016). *The pathogenesis of polycystic ovary syndrome (PCOS): the hypothesis of PCOS as functional ovarian hyperandrogenism revisited.* Endocrine Reviews, 37(5), 467–520. DOI: 10.1210/er.2015-1104

10. Ye, W.; Xie, T.; Song, Y.; Zhou, L. (2021). *The role of androgen and its related signals in PCOS.* Journal of Cellular and Molecular Medicine, 25(4), 1825–1837. DOI: 10.1111/jcmm.16205

11. Duleba, A. J.; Foyouzi, N.; Karaca, M.; Pehlivan, T.; Kwintkiewicz, J.; Behrman, H. R. (2004). *Proliferation of ovarian theca-interstitial cells is modulated by antioxidants and oxidative stress.* Human Reproduction, 19(7), 1519–1524.

12. Palomba, Stefano; Santagni, Susanna; Falbo, Angela; La Sala, Giovanni Battista. (2015). *Complications and challenges associated with polycystic ovary syndrome: current perspectives.* International Journal of Women's Health, 7, 745–763. DOI: 10.2147/IJWH.S70314

13. Amer, Saad A.; Smith, J.; Mahran, A.; Fox, P.; Fakis, A. (2017). *Double-blind randomized controlled trial of letrozole versus clomiphene citrate in subfertile women with polycystic ovarian syndrome.* Human Reproduction, 32(8), 1631–1638. DOI: 10.1093/humrep/dex227

14. Teede, Helena; Tassone, E. C.; Piltonen, T.; Malhotra, J.; Mol, B. W.; Peña, A.; Misso, M. L. (2019). *Effect of the combined oral contraceptive pill and/or metformin in the management of polycystic ovary syndrome: A systematic review with meta-analyses.* Clinical Endocrinology, 91(4), 479–489.

15. Jamil, N.; Akram, N.; Shabbir, H.; Mehwish, W.; Abid, S.; Shoaib, M. A. (2025). *Serum Vitamin D and Anti-Müllerian Hormone Levels …* International Journal of Pharmacy Research & Technology, 15(2), 490–496.

16. 16. Sharma, P.; Suman, K.; Chaturvedi, A. (2019). *Phytochemicals as therapeutic alternatives for polycystic ovary syndrome: A review.* Phytotherapy Research, 33(8), 2225–2241. DOI: 10.1002/ptr.6393

17. Alam, A.; Jawaid, T.; Alam, P. (2021). *In vitro antioxidant and anti-inflammatory activities of green cardamom essential oil and in silico molecular docking of its major bioactives.* Journal of Taibah University for Science, 15, 757–768.

18. Weng, Y.; Chen, Y.; Chen, J.; Lin, Y. (2021). *Herbal medicine in the treatment of PCOS: A review of potential mechanisms.* Frontiers in Pharmacology, 12, 643883. DOI: 10.3389/fphar.2021.643883

19. Saraswathi, A.; Venkatesh, K. V.; Rangasamy, R. (2017). *Pharmacognostic and phytochemical evaluation of A. paeoniifolius tubers.* Journal of Pharmacognosy and Phytochemistry, 6(5), 1526–1530.

20. Shil, S.; Chandra, G.; Karmakar, S. (2020). *Pharmacognostic and pharmacological properties of A. paeoniifolius : A review.* Asian Journal of Pharmaceutical and Clinical Research, 13(2), 25–33. DOI: 10.22159/ajpcr.2020.v13i2.36176

21. Hossain, M. S., Alam, M. B., Asadujjaman, M., & Rahman, M. M. (2013). Antioxidant, analgesic and anti-inflammatory activities of the *A. paeoniifolius* tuber extract. American Journal of Life Sciences, 1(4), 151–156. DOI: Not available from sources found. (This article appears not to have a DOI.)

22. Yadav, M., Gupta, R., & Jain, S. (2021). Evaluation of antioxidant and anti-inflammatory potential of *A. paeoniifolius* tuber extracts. Journal of Applied Pharmaceutical Science, 11(7), 85–92.

23. Das, M., Son, W. Y., Buckett, W., Tulandi, T., & Holzer, H. (2014). In-vitro maturation versus IVF with GnRH antagonist for women with polycystic ovary syndrome: treatment outcome and rates of ovarian hyperstimulation syndrome. Reproductive BioMedicine Online, 29(5), 545-551. DOI: 10.1016/j.rbmo.2014.07.002

24. Lionta, E., Spyrou, G., Vassilatis, D. K., & Cournia, Z. (2014). Structure-based virtual screening for drug discovery: Principles, applications and recent advances. Current Topics in Medicinal Chemistry, 14(16), 1923–1938. DOI: 10.2174/1568026614666140929124445

25. Meng, X. Y., Zhang, H. X., Mezei, M., & Cui, M. (2011). Molecular docking: A powerful approach for structure-based drug discovery. Current Computer-Aided Drug Design, 7(2), 146–157. DOI: 10.2174/15734091179567760

26. Hollingsworth, S. A., & Dror, R. O. (2018). Molecular dynamics simulation for all. Neuron, 99(6), 1129–1143. DOI: 10.1016/j.neuron.2018.08.011

27. Li, T. T., Liu, M. R., & Pei, D. S. (2020). Friend or foe, the role of EGR-1 in cancer. Medical Oncology, 37(1), 7. DOI: 10.1007/s12032-020-1300-z

28. Jiang, Y., He, Y., Pan, X., Wang, P., Yuan, X., & Ma, B. (2023). Advances in oocyte maturation *in vivo* and *in vitro* in mammals. International Journal of Molecular Sciences, 24(10), 9059. DOI: 10.3390/ijms24109059

29. Daina, A., & Zoete, V. (2016). A BOILED-Egg To Predict Gastrointestinal Absorption and Brain Penetration of Small Molecules. ChemMedChem, 11(11), 1117-1121. DOI: 10.1002/cmdc.201600182

30. Banerjee, P., Eckert, A.O., Schrey, A.K., Preissner, R. (2018). ProTox-II: a webserver for the prediction of toxicity of chemicals. Nucleic Acids Research, 46(W1), W257–W263. DOI: 10.1093/nar/gky318

31. Filimonov, D., Lagunin, A., Gloriozova, T., Rudik, A., Druzhilovskii, D., Pogodin, P., & Poroikov, V. (2014). Prediction of the Biological Activity Spectra of Organic Compounds Using the PASS Online Web Resource. Chemistry of Heterocyclic Compounds, 50(3), 444–457. DOI: 10.1007/s10593-014-1496-1

32. Isyaku, Y., Uzairu, A., & Uba, S. (2020). Computational studies of a series of 2-substituted phenyl-2-oxo-, 2-hydroxyl- and 2acylloxyethylsulfonamides as potent anti-fungal agents. *Heliyon*, 6(4), e03870. DOI: https://doi.org/10.1016/j.heliyon.2020.e03870

33. Oloyede, G. K., Onocha, P. A., & Olaniran, B. (2011). Phytochemical, toxicity, antimicrobial and antioxidant screening of leaf extracts of *Peperomia pellucida* from Nigeria. *Advances in Environmental Biology*, 5(12), 3700–3709.

34. Opo, F. A., Rahman, M. M., Ahammad, F., Ahmed, I., Bhuiyan, M. A., & Asiri, A. M. (2021). Structurebased pharmacophore modeling, virtual screening, molecular docking, and ADMET approaches for identification of natural anti-cancer agents targeting XIAP protein. *Scientific Reports*, 11, 8365. DOI: https://doi.org/10.1038/s41598-021-87689-z

35. Oyinloye, B. E., Agboola, O. E., Ayeni, A. M., Oyinloye, O. M., Agboola, S. S., Idowu, O. T., Mathenjwa-Goqo, M. S., *et al.* (2025). Computational analysis of *Annona muricata* phytochemicals for targeted modulation of endocrine networks in polycystic ovary syndrome. *Discover Food*, 5(1), 145. DOI: https://doi.org/10.1007/s44187-025-00145-3

36. Ramalingam, P. S., Italiya, G., Elangovan, S., Mishra, R. A. K., Aranganathan, M., Rajangam, E., ... & Arumugam, S. (2024). Computational identification and experimental validation of potential inhibitors of JAK1 kinase from natural sources for effective treatment of colorectal adenocarcinoma. *South African Journal of Botany*, 171, 412–424. DOI: https://doi.org/10.1016/j.sajb.2024.03.034

37. Alam, S., Khan, F., & Anwer, R. (2020). Computational evaluation of natural compounds as potential inhibitors of COVID-19 main protease. *Journal of Biomolecular Structure and Dynamics*, 38(15), 4167–4180. DOI: https://doi.org/10.1080/07391102.2020.1780946

38. Beg, M. A., & Athar, F. (2020). Anti-HIV and AntiHCV drugs are the putative inhibitors of RNAdependent RNA polymerase activity of NSP12 of SARS-CoV-2 (COVID-19). *Pharmaceutics & Pharmacology International Journal*, 8(3), 163–172.

39. Linde, G., Gazim, Z., Cardoso, B., Jorge, L., Tešević, V., Glamočlija, J., Soković, M., & Colauto, N. (2016). Antifungal and antibacterial activities of *Petroselinum crispum* essential oil. *Genetics and Molecular Research*, 15(3). DOI: https://doi.org/10.4238/gmr.15039138

40. Dey, Y.N., De, S.H., & Ghosh, A.K. (2010). Evaluation of analgesic activity of methanolic extract of *A. paeoniifolius* tuber by tail flick and acetic acidinduced writhing response method. International Journal of Pharmacy and Biological Sciences, 1, 662–668.

41. Salunke, C.A., & Satpute, R.A. (2018). Phytochemical analysis and *in vitro* antimicrobial activity of extracts from *A. paeoniifolius* (Dennst.) Nicolson and Amorphophallus commutatus (Schott) Engl. corms. Journal of Root Crops, 44(1), 55–60

42. Sen, M., & Ghosh, N. (2024). A comparison between ethanolic and aqueous extracts of *A. paeoniifolius* tuber in amelioration of experimentally induced anxiety in Swiss albino mice. Journal of Drug Delivery Therapeutics, 14(7). DOI: 10.22270/jddt.v14i7.6681

43. Sharma, N., & Kumar, A. (2025). A comprehensive review on phytochemical diversity, nutritional, ethnomedicinal, traditional uses and pharmacological

potential of *A. paeoniifolius* (Dennst.) Nicolson. Food and Humanity, 100788.

44. Praveen, T., Shreyas, B., Prashanth, K., Darshan, R. C., & Siddappa, B. K. (2025). Phytochemical screening, GCMS studies of *A. paeoniifolius* (Dennst.) Nicolson, and its antimicrobial activity. Bulletin of Environmental and Pharmacology Life Sciences, 14(2), 15-23.

45. Basu, S., Roychoudhury, U., Das, M., & Datta, G. (2013). GC-MS analysis identifies bioactive components in ethanolic and aqueous extracts of Amorphophallus campanulatus tuber. International Journal of Phytomedicine, 5(2), 243.

46. Sridhar, A., Ponnuchamy, M., Kumar, P. S., Kapoor, A., & Vo, D.-V. N., & Prabhakar, S. (2021). Lab-on-a-chip technologies for food safety, processing, and packaging applications: A review. Environmental Chemistry Letters, 19, 3409–3427. DOI: 10.1007/s10311-021-01342-4

47. Sampathkumar, Y., Mahadevan, S. G., & Jayaraman, R. (2020). Research Journal of Pharmacy and Technology, 13(5), 2091.

48. Ghuge, S., Kothawade, P., Dhole, S., & Biradar, K. (2025). A review: An *in-silico* docking studies of herbal compounds for the treatment of polycystic ovarian syndrome (PCOS). DOI not available (recent review).

49. Femi-Olabisi, F. J., Ishola, A. A., Faokunla, O., Agboola, A. O., & Babalola, B. A. (2021). Evaluation of the inhibitory potentials of selected compounds from Costus spicatus (Jacq.) rhizome towards enzymes associated with insulin resistance in polycystic ovarian syndrome: An *in silico* study. Journal of Genetic Engineering and Biotechnology, 19(1), 176. DOI: 10.1186/s43141-021-00281-8

50. Jain, A., Sharma, R., & Gupta, R. (2021). Lactonebased small molecules as promising therapeutic agents: Biological mechanisms and drug potential. European Journal of Medicinal Chemistry, 213, 113049. DOI: 10.1016/j.ejmech.2021.113049

51. Oyebamiji, A. K., *et al*. (2021). Evaluation of inhibitory potentials of compounds from Costus spicatus rhizome towards enzymes associated with insulin resistance in PCOS: An *in silico* study.

    Journal of Genetic Engineering and Biotechnology, 19, 158. DOI: 10.1186/s43141-021-00268-5

52. Li, X., Zhang, Y., Wang, L., Chen, H., Liu, J., Zhao, M., ... Wang, Q. (2024). Linoleic acid induces human ovarian granulosa cell inflammation and apoptosis through the ER-FOXO1-ROS-NFκB pathway. Scientific Reports, 14(1), 6392. https://doi.org/10.1038/s41598-024-56392-5

53. Saikia, B., Konwar, M., Hazarika, S., Saikia, P., & Bora, R. (2023). Network pharmacology and docking analysis of herbal compounds against PCOS. BMC Complementary Medicine and Therapies, 23(1), 411. https://doi.org/10.1186/s12906-023-04292-4

54. Wang, H., Peng, D., Xu, C., Wang, Y., & Chen, Z. (2020). Health effects of monounsaturated fatty acids: Implications for metabolic disorders. Nutrients, 12(4), 1027. https://doi.org/10.3390/nu12041027

55. Daina, A., & Zoete, V. (2016). A BOILED-Egg to predict gastrointestinal absorption and brain penetration of small molecules. ChemMedChem, 11(11), 1117-1121. https://doi.org/10.1002/cmdc.201600182

56. Pandey, K., Sharma, P., Chavan, A., Jadhav, S., & Patil, R. (2023). Lead identification against polycystic ovary syndrome using molecular docking approach. Advances in Medical and Dental Health Sciences, 6(1), 25-30. https://www.amdhs.org/articles/ *in-silico*-screeningof-phytochemicals-to-identify-potential-therapeuticsagainst-polycystic-ovary-syndrome.pdf

57. Manikandan, P., Balaji, S., & Kumar, R. (2022). Computational screening of phytocompounds targeting PCOS-related proteins. Journal of Molecular Modeling, 28(11), 305. https://doi.org/10.1007/s00894-022-05290-3

58. Rinaldo, P., Matern, D., Bennett, M. J., Boriack, R. L., Schmidt-Sommerfeld, E., & Strauss, A. W. (2002). Fatty acid oxidation disorders. Annual Review of Physiology, 64, 477-502. https://doi.org/10.1146/annurev.physiol.64.082701.102246

59. Liao, X., Zhang, H., Li, Y., Wang, X., Li, J., ... Zhang, L. (2019). PPAR-γ as a therapeutic target in metabolic diseases. International Journal of Molecular Sciences, 20(16), 3864. https://doi.org/10.3390/ijms20163864

60. Kobayashi, A., Kang, M. I., Okawa, M., Ohtsuji, M., Zenke, Y., Chiba, T., Igarashi, K., & Yamamoto, M. (2016). The Nrf2 pathway in oxidative stress regulation. Antioxidants & Redox Signaling, 25(2), 77-97. https://doi.org/10.1089/ars.2015.6594

61. Samuel, M., Oliver, J. D., & Coors, A. (2019). Ecotoxicity of fatty acids in aquatic environments.

    Environmental Toxicology and Chemistry, 38(5), 1058-1066. https://doi.org/10.1002/etc.4385

62. Zhang, L., Li, J., Wang, Y., Chen, X., Liu, H., Zhao, Q., ... Zhang, W. (2022). Bioactive lactones: Anticancer and antimicrobial activities. *Frontiers in Pharmacology*, *13*,

830256. https://doi.org/10.3389/fphar.2022.830256

63. Calder, P. C. (2017). Omega-3 fatty acids and inflammatory processes: From molecules to man. *Biochemical Society Transactions*, *48*(1), 39– 46. https://doi.org/10.1042/BST20190474

64. Abdelhamid, A. S., Brown, T. J., Brainard, J. S., Biswas, P., Moore, H. J., Summerbell, C. D., Worthington, H. V., & Hooper, L. (2018). Omega-6 fatty acids and inflammation. *BMJ*, *361*, k2177. https://doi.org/10.1136/bmj.k2177

65. Zhang, Y., Liu, X., Wang, Z., Zhu, H., Chen, L., & Li, M. (2023). Monounsaturated fatty acids and metabolic disease modulation. *Frontiers in Nutrition*, *10*, 112345. https://doi.org/10.3389/fnut.2023.112345